Bull. Mater. Sci., Vol. 29, No. 3, June 2006, pp. 317–322. © Indian Academy of Sciences.

Optical, structural and electrical properties of Mn doped tin oxide thin films

RAJEEB BRAHMA, M GHANASHYAM KRISHNA* and A K BHATNAGAR[†]
School of Physics, University of Hyderabad, Hyderabad 500 046, India
[†]Also at Pondicherry University, Pondicherry Central University PO, Pondicherry 605 014, India

MS received 13 January 2006; revised 3 April 2006

Abstract. **Mn doped SnO_x thin films have been fabricated by extended annealing of Mn/SnO_2 bilayers at 200°C in air for 110 h. The dopant concentration was varied by controlling the thickness of the metal layer. The overall thickness of the film was 115 nm with dopant concentration between 0 and 30 wt% of Mn. The films exhibit nanocrystalline size (10–20 nm) and presence of both SnO and SnO_2. The highest transmission observed in the films was 75% and the band gap varied between 2·7 and 3·4 eV. Significantly, it was observed that at a dopant concentration of ~ 4 wt% the transmission in the films reached a minimum accompanied by a decrease in the optical band gap. At the same value of dopant concentration the resistivity also reached a peak. This behaviour appears to be a consequence of valence fluctuation in Sn between the 2+ and 4+ states. The transparent conductivity behaviour fits into a model that attributes it to the presence of Sn interstitials rather than oxygen vacancies alone in the presence of Sn^{2+}.**

Keywords. **Tin oxide; transparent conductors; thin films.**

1. Introduction

Transparent conducting oxides have been the subject of research interest over a number of years (Gordon 2000; Kikuchi *et al* 2002; Man-Soo *et al* 2003; Matsubara *et al* 2003; Wohlmuth and Adesida 2005). SnO_2 based systems, in particular, have been the focus of many of these investigations. SnO_2 evinces interest because it is a naturally non-stoichiometric prototypical transparent conducting oxide. It has a high band gap of almost 4 eV, plasma frequency in the IR region and, when suitably doped, can be used both as a *p*-type and *n*-type semiconductor. It crystallizes in the tetragonal rutile type of structure, D_{4h}^{14} ($P4_2/mnm$) with two Sn and four oxygens per unit cell. The lattice parameters are $a = b = 0·4737$ nm, $c = 0·3185$ nm and $c/a = 0·673$.

Thin films of pure and doped SnO_2 have been deposited by various physical and chemical methods (Brousse and Schleich 1996; Cirilli *et al* 1998; Dhere *et al* 1998; Mientus and Ellmer 1998; Yan *et al* 1998; Bauduin *et al* 1999; Jae-Ho *et al* 1999; Shokr *et al* 2000; Robbins *et al* 2001; Shamala *et al* 2004). It is evident from literature that most of the focus of interest in doped SnO_2 based thin films has been on the $SnO_2:F$ and $SnO_2:Sb$ systems and there is scattered literature on dopants such as Nb (Kikuchi *et al* 2002), Al (Bagheri-Mohagheghi and Shokooh-Saremi 2004), Mo (Sterna and Granqvist 1994) and In (Enoki 1991). There is not much work known on other metal doped SnO_2 thin films. In this paper, therefore, we have investigated the transparency and conductivity in the Mn–SnO_2 series of thin films as possible candidates for *p*-type transparent conducting thin films. Thin films were fabricated by thermal evaporation from a resistive source in the case of the metal and a W boat in the case of the oxide. Thin films were characterized for transmission in the range, 190–2500 nm, resistivity using four-probe method, microstructure by atomic force microscopy and structure using X-ray diffraction.

2. Experimental

Metal-doped SnO_2 films were deposited by thermal evaporation on borosilicate glass substrates. A constant pressure of $5·0 \times 10^{-6}$ Torr was maintained during the deposition process. Mn (99·9% purity) was first deposited on the borosilicate glass substrates and the SnO_2 film was deposited sequentially on top of the metal films. The weight of metals in each deposition was maintained same. SnO_2 powder of 99·9% purity and weight, 0·1150 g, was used in each deposition. Deposition rate of the films estimated from the thickness of the films was 2~3 Å/S. Films were then annealed in a furnace at 200°C for 110 h continuously. The resistance of the films was measured in 12 h intervals in order to note the variation of resistance with the annealing time and annealing was stopped after the resistance saturated at a particular value.

*Author for correspondence (mgksp@uohyd.ernet.in)

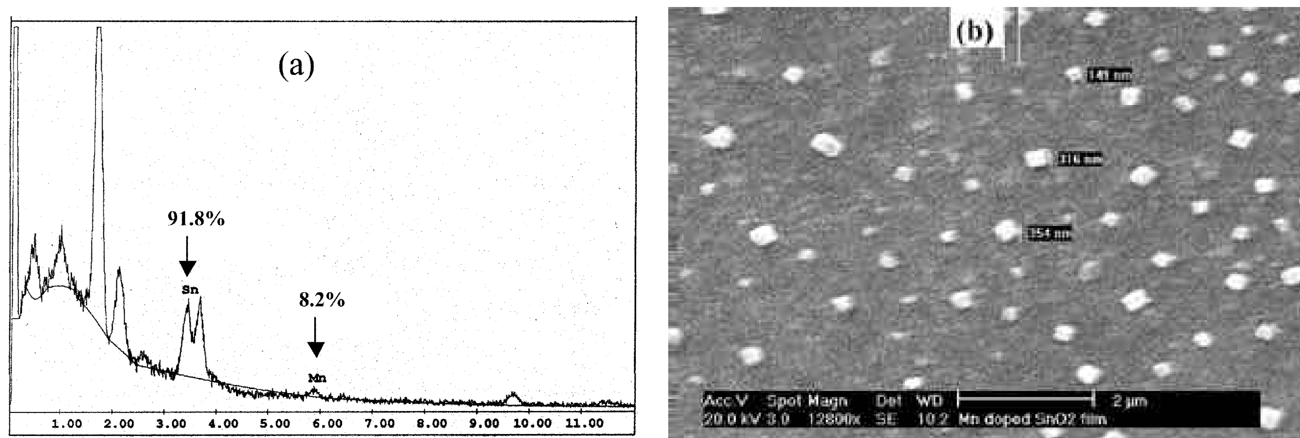

Figure 1. Typical (**a**) EDAX and (**b**) SEM picture of Mn doped SnO_2 thin film.

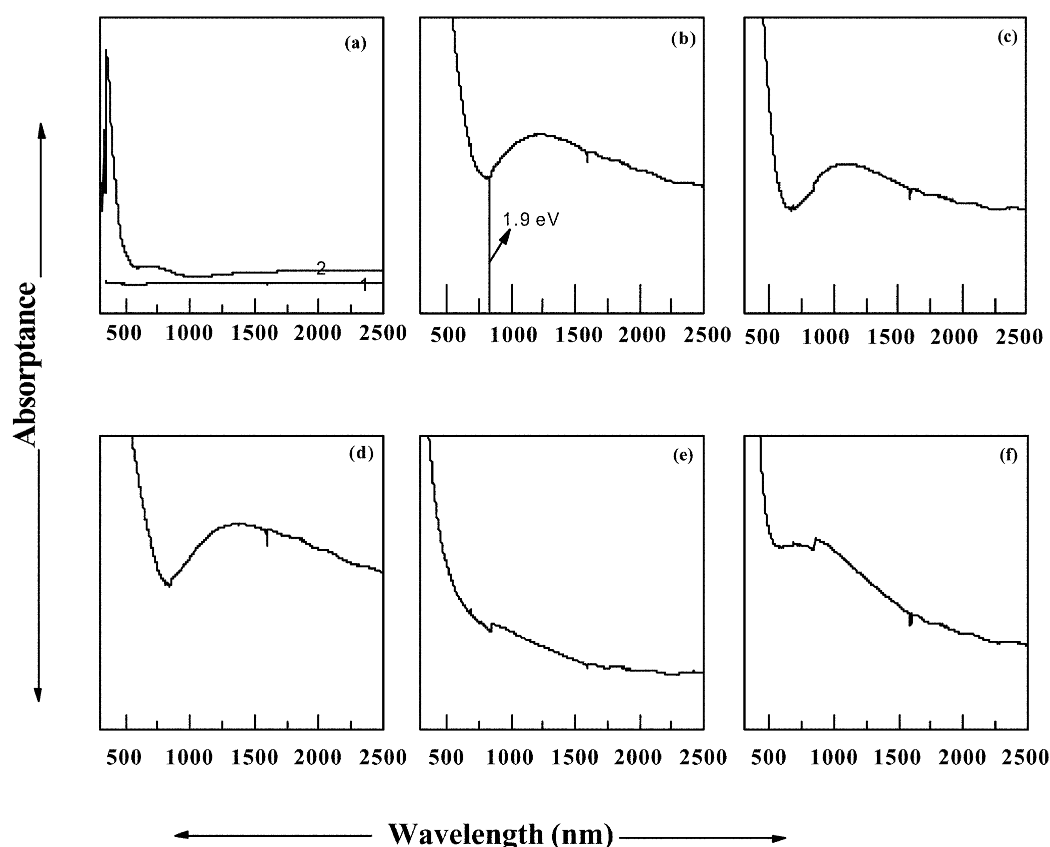

Figure 2. Optical absorption spectrum of (**a**) bare glass (1), pure SnO_2 film (2) and Mn doped SnO_2 thin film with Mn concentration of (**b**) 8·2 wt%, (**c**) 14 wt%, (**d**) 20 wt%, (**e**) 27·5 wt% and (**f**) 29·2 wt%.

The thickness of the films was measured with stylus surface profilometer (Model XP1 of Ambios Technology, USA). Structural analysis of the films were carried out using X-ray diffraction with Co K_{α} (λ = 1·7889 Å) radiation in a wide angled powder X-ray diffractometer (INEL Model CPS 120). The crystallite sizes, d, were determined by using Scherrer's formula ($d = k\lambda/\beta\cos\theta$), where k is a constant = 0·9, β is the FWHM and θ the angle at which the peak occurs. Chemical compositions of the films were determined by EDAX (PHILIPS XL 30 series environmental SEM at an accelerating voltage of 20 kV mode). Optical transmission of the films in the range 190–2500 nm was measured by using a JASCO V 570 UV–VIS–NIR spectrophotometer. Microstructure of the films were stu-

died by atomic force microscopy operating in the non-contact DFM mode (SPA 400 of Seiko Instruments Inc., Japan with SPI–3800 probe station). Resistivity measurements were carried out using a spring-loaded collinear four-point probe, using a current source and voltmeter (Model 225 current source and 195 system DMM of M/s Keithley instruments, USA).

3. Results and discussion

The first analysis done on the films was to establish that doping had indeed taken place and the films were not composites of the metal and tin oxide. EDAX experiments done on these films clearly showed that the grains were typically comprised of both Mn and Sn metals. A typical EDAX spectrum and the corresponding SEM image are shown in figures 1(a) and (b), respectively. Secondly, optical absorption spectra were taken for the films and are shown in figure 2. From these figures it is evident that there are three features in the absorption spectra present in majority of the films. Furthermore, it is evident while the features at 1400 and 2000 nm are from the BSG substrate, the feature at 1·90 eV (650 nm) is neither due to the substrate nor is it due to SnO_2 and it can be assigned to Mn^{2+} ions in the lattice (Mochizuki 1990). There is a shift in the wavelength at which it occurs clearly signifying a crystal field effect. Further evidence is presented in the form of X-ray diffraction patterns shown in figure 3. From this figure it is observed that the peaks in the doped films shift from their standard positions in the presence of the dopant. The shift in the lattice parameter is mainly due to the dopant occupying interstitial positions in the lattice. Hence from the EDAX, optical absorption spectra and X-ray diffraction patterns, it is clear that the Mn^{2+} ions are acting as dopants in the SnO_2 structure.

The X-ray diffraction patterns also indicate that the films dissociate partly into SnO and SnO_2 resulting in non-stoichiometry. The amount of non-stoichiometry and therefore, the number of Sn^{2+} ions in the lattice is a function of the dopant concentration. There was complete absence of reflections from the metal dopant confirming that the metal particles were nano-crystalline within the detectable limits. There was also no evidence for the formation of solid-solution from the X-ray diffraction patterns. SnO_2 films with up to 10 wt% dopant have been observed to exhibit the absence of dopant peaks (Shanti *et al* 1980). In our study this was true even at concentration as high as 40%.

Figures 4(a) and (b) show transmission at 800 nm, the optical band gap and resistivity of the films as a function of dopant concentration. All films exhibited resistivity in the range 10^{-2} ohm-cm. The resistivity was dependent on dopant concentration and similar oscillatory behaviour in resistivity has been observed in the case of Sb doped SnO_2 thin films prepared by spray pyrolysis (Elangovan *et al* 2004). In that work the variation has been related to the increase in mobility at a particular concentration. Other work on Nb (Kikuchi *et al* 2002) and Al (Bagheri-Mohagheghi and Shokooh-Saremi 2004) doped SnO_2 thin films also report similar resistivity behaviour.

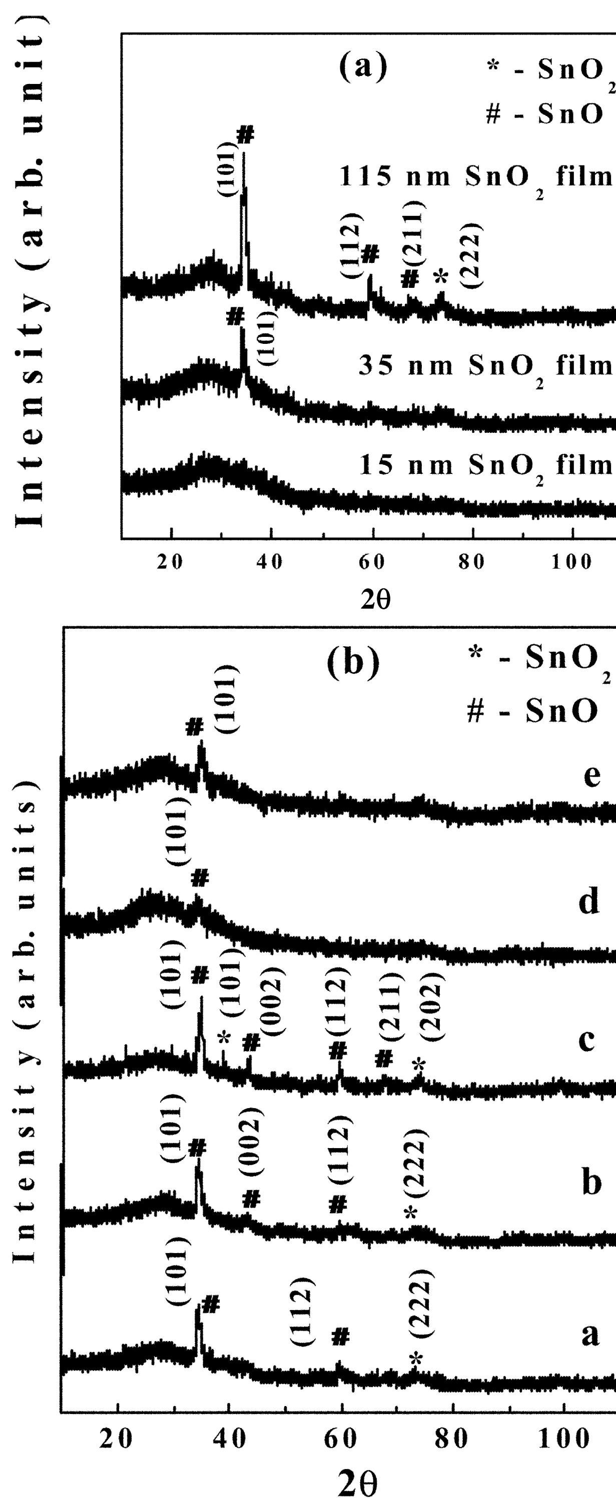

Figure 3. XRD patterns of (a) pure SnO_2 thin film and (b) Mn doped SnO_2 films with Mn concentration of (**a**) 8·2 wt%, (**b**) 14 wt%, (**c**) 20 wt%, (**d**) 27·5 wt% and (**e**) 29·2 wt%.

The morphology of the films was studied by AFM. It was found that for lower dopant concentration, films were non-uniform. As the dopant concentration was increased, the films became denser and closely packed. The average particle size measured for lower concentrations was found to be 50 nm as shown in figure 5 and for higher dopant concentration it was found to be 60–70 nm. This clearly indicates that the metal dopant inhibits grain growth. The microstructural images taken for all doped samples revealed that the grain sizes in general were smaller than those for the undoped samples. They also revealed that doped films were denser with more uniform spherical grains. The films exhibit nanocrystalline size in the range of 10–20 nm as derived from X-ray diffraction patterns.

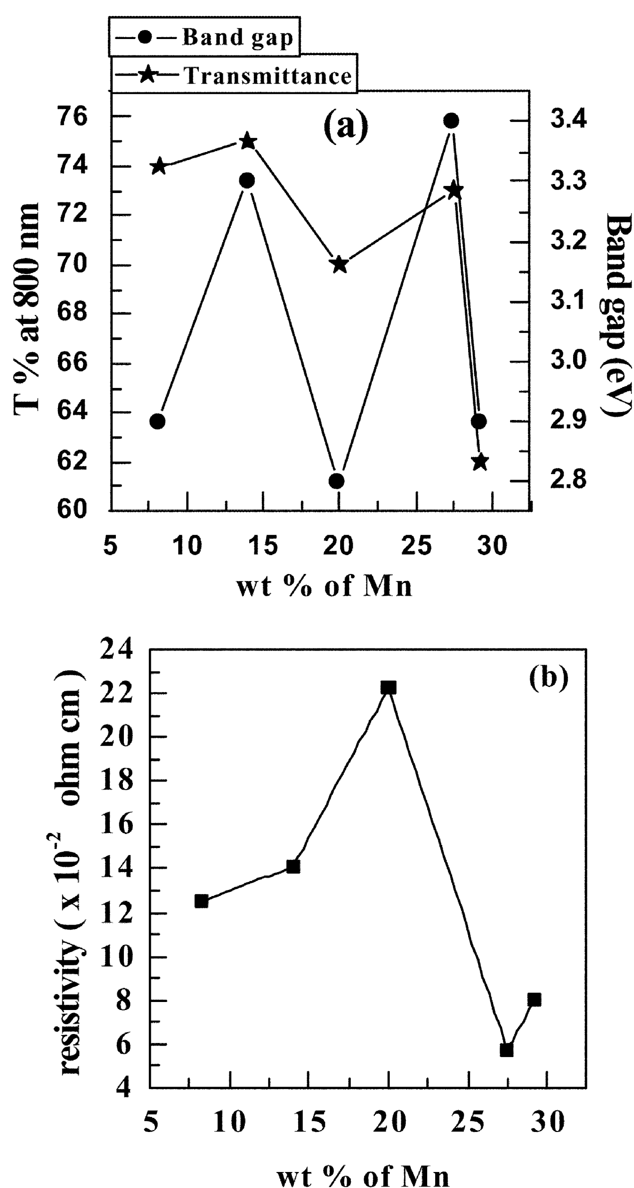

Figure 4. (**a**) Transmission at 800 nm as a function of dopant concentration of Mn and (**b**) resistivity as a function of dopant concentration of Mn. [The connecting lines are only a guide for the eye].

It is clear that the doped SnO_2 films in the current study exhibit the properties of transparency and semiconductivity. The transparency of the SnO_2 matrix increased with the introduction of dopants and this was independent of dopant and accompanied by an increase in conductivity. Similar observations have been made on Sb doped SnO_2 films (Shanti *et al* 1980; Nakanishi *et al* 1991; Shokr *et al*

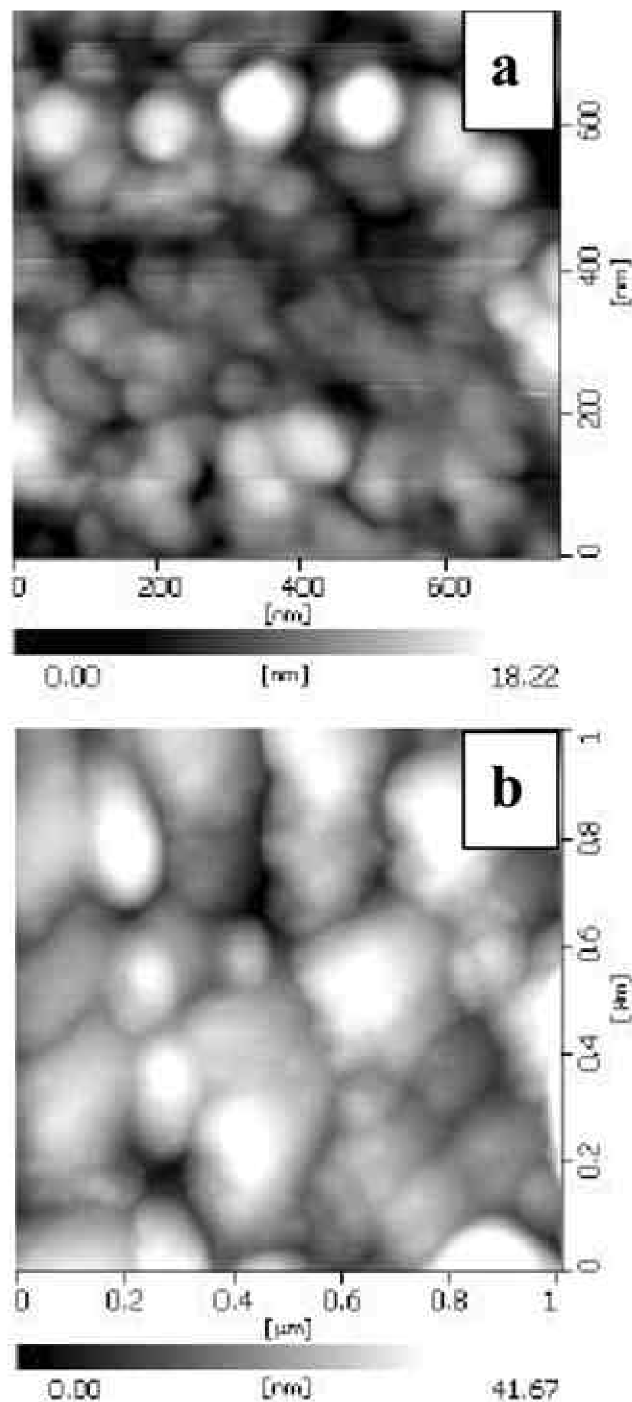

Figure 5. AFM pictures of (**a**) pure SnO_2 and (**b**) Mn doped SnO_2 thin films.

2000; Jin *et al* 2002). It is significant that the minimum in transmittance and band gap and the peak in resistivity, all appear at the same dopant concentration. In addition, X-ray diffraction patterns indicate the presence of SnO that points to the fact that the peak in resistivity is caused by valence fluctuation between the Sn^{2+} and Sn^{4+} state in the presence of dopant (Pan and Fu 2001). The presence of Sn^{2+} ions can be attributed to the evaporation process itself. The increased oxygen vacancies and defects at low dopant concentration increase conductivity initially. Further increase in dopant concentration increases the Sn^{2+} concentration as will be discussed below. Sb doped SnO_2 films have been reported to exhibit a peak in resistivity at ~ 10 wt% (Shanti *et al* 1980). The conductivity behaviour is, however, oscillatory indicating that several competing mechanisms are operating, these dominate depending on the level of dopant concentration.

Based on a local density approximation (LDA) (Cetin and Zunger 2002), it has been found that the Sn interstitial defects play a more important role in conduction than oxygen vacancies. It was proposed that tin interstitials produce a donor level inside the conduction band due to their loosely bound outer electrons which gives rise to donor ionization and conductivity. Oxygen vacancies on the other hand would tend to produce deep levels inside the band gap. Sn interstitials have a very low formation energy, therefore, they can exist in significant quantities and they are stable due to the intrinsic multivalency of Sn. It was shown that the presence of Sn interstitial lowers the formation energy of oxygen vacancy that in turn results in the natural oxygen deficiency and nonstoichiometry of SnO_2. The absence of inter-conduction-band absorption is a consequence of a special feature of the band structure of SnO_2, manifesting as a large internal gap inside the conduction band that eliminates optical transitions in the visible range. The lowest direct optical transition corresponds to energy above 3·7–4·0 eV. The indirect transitions dominate as Sn^{2+} increases in the system and occurs within the conduction band at 2·7–3·1 eV causing transparency in the visible range. Furthermore, the conduction band absorption remains small, so the optical transparency is maintained even in the presence of intrinsic defects. Another important feature of the SnO_2 electronic structure is that the Fermi level lies deep inside the conduction band. As non-stoichiometry is introduced in the system, either intrinsically or as a consequence of doping, the Fermi level is suppressed and eventually shifts to just below the conduction band or above the valence band depending on the nature of dopant (Shanti *et al* 1980). Significantly, as predicted by the LDA calculations, it is seen from figures 4(a) and (b), that the minimum transmittance and the band gap occur at the same dopant concentration. Secondly, the value of the band gap is in the range 2·7–3·1 eV, which indicates the presence of Sn^{2+} ions. This is clearly in conformity with the theory discussed above. It should be noted that the arguments for variation in resistivity behaviour of Sb doped SnO_2 films focus mainly on valence fluctuations of the dopant and not Sn. This is because the films in those cases are stoichiometric or even mildly non-stoichiometric. In the present case valence fluctuations in Sn are considered since structural evidence points to the presence of Sn^{2+} in all the films.

4. Conclusions

Transparent conducting oxide thin films in the $Mn:SnO_2$ series have been demonstrated. The transparency is ~ 80% for the best films with resistivity of the order of 10^{-2} ohm-cm. The behaviour of the films has been explained within the framework of current models for the coexistence of transparency and conductivity in SnO_2 based systems.

Acknowledgements

The authors acknowledge support from the DST-ITPAR, DST-FIST, UPE, SAP and NPSM programs. One of the authors (RB) acknowledges financial support from the NPSM project.

References

Bagheri-Mohagheghi M M and Shokooh-Saremi M 2004 *Appl. Phys.* **37** 1248

Bauduin N, Hellegouarc F, Planade R, Amouroux J and Arefi-Khonsari F 1999 in *Proceedings of the international symposium on plasma chemistry (ISPC)* (Czech Republic: Institute of Plasma Physics) Vol. IV, p. 1457

Brousse T and Schleich D M 1996 *Sensors & Actuators* **B31** 77

Cetin K and Zunger A 2002 *Phys. Rev. Lett.* **88** 095501

Cirilli F, Kaciulis S, Mattogno G, Galolikas A, Mironas A, Senuliene D and Setkus A 1998 *Thin Solid Films* **315** 310

Dhere R G, Moutinho H R, Asher S, Young D, Li X, Ribelin R and Gessert T 1998 *Proc. of national centre for photovoltaics program review meeting*, NREL/CP-520-25733

Elangovan E, Ramesh K and Ramamurthi K 2004 *Solid State Commun.* **130** 523

Enoki H 1991 *J. Mater. Sci. Lett.* **10** 970

Gordon R G 2000 *MRS Bull.* **25** 56

Jae-Ho C, Yong-Sahm C and Dae-Seung K 1999 *Thin Solid Films* **349** 126

Jin M, Xxiaotao H, Honglei M, Xiangang X, Yingge Y, Huang S, Zhang D and Cheng C 2002 *Solid State Commun.* **121** 345

Kikuchi N, Kusano E, Kishio E and Kingara A 2002 *Vacuum* **66** 365

Man-Soo H, Lee H J, Jeong H S, Seo Y W and Kwon S J 2003 *Surf. & Coat. Technol.* **29** 171

Matsubara K, Fons P, Iwata K, Yamada A, Sakurai K, Tampo H and Niki S 2003 *Thin Solid Films* **431–432** 369

Mientus R and Ellmer K 1998 *Surf. & Coat. Technol.* **98** 1267

Mochizuki S 1990 *J. Phys.: Condens. Matter* **2** 7225

Nakanishi Y, Suzuki Y, Nakamura T, Hatanaka Y, Fukuda Y, Fujisawa A and Shimaoka G 1991 *Appl. Surf. Sci.* **48/49** 55

Pan X Q and Fu L 2001 *J. Appl. Phys.* **89** 6048

Robbins J J, Alexander R T, Mailasu B, Yen-Jung H, Tyrone L Vincent and Wolden C A 2001 *J. Vac. Sci. Technol*. **A19** 2766
Shamala K S, Murthy L C S and Narasimha Rao K 2004 *Bull. Mater. Sci*. **27** 295
Shanti E, Dutta V, Banerjee A and Chopra K L 1980 *J. Appl. Phys*. **51** 6243
Shokr E K, Wakkad M M, Abd El-Ghanny H A and Ali H M 2000 *J. Phys. Chem. Solids* **61** 75
Sterna B and Granquist C G 1994 *J. Appl. Phys*. **76** 3797
Wohlmuth W and Adesida I 2005 *Thin Solid Films* **479** 223
Yan H, Chen G H, Man W K, Wong S P and Kwok R W M 1998 *Thin Solid Films* **326** 88